



## Characterization of Photo-Neutrons Produced by 150 MeV and 1 GeV Electrons Impinging on High Z-Metallic Targets for Neutron Resonance Spectroscopy

ElTayeb ElSaady<sup>1</sup>, Mustafa M. M. ElAshmawy<sup>1</sup>, Hosnia M. Abu-Zeid<sup>2</sup>, Afaf A. Nada<sup>2</sup>, Fatma ElZahraa M. Ragab<sup>2</sup>

<sup>1</sup> Egyptian Nuclear and Radiological Regulatory Authority, Cairo, Egypt

<sup>2</sup> Faculty of women for Arts, Sci. and Education, Ain Shams University, Cairo, Egypt

Received 7<sup>th</sup> May 2018  
Accepted 17<sup>th</sup> Mar. 2019

Monte Carlo calculations have been performed using MCNP code to study the generation, angular distribution and energy spectrum of photo-neutrons for 1 GeV and 150 MeV electron beam energies impinging on different thickness of Tungsten, Tantalum and Lead targets. It is noticed that the photo-neutron yield increases as the target thickness increases, then saturates beyond an optimized thickness of the target. Moreover, the photo-neutron yield shows a significant increase as the electron energy increases. At the optimized thickness, the angular distribution of photo-neutrons is found almost isotropic for 150 MeV electrons and anisotropic for 1 GeV electrons. Furthermore, by increasing the electron energy and/or the target thickness, the angular distribution is found to be forward peaked. The energy spectrum of photo-neutrons can be well described by a Maxwellian distribution for both electron energies. Such calculations can help in developing a photo-neutron source-based time of flight facility (TOF) for elemental and isotopic identification via neutron resonance spectroscopy. Photo-neutron yields, angular distribution, mean energy, energy spectrum and nuclear temperature for 1 GeV and 150 MeV electron energies and different target materials are presented.

**Keywords:** Photo-neutron, Angular distribution, Monte Carlo calculations, Electron accelerator

### Introduction

In earlier works, the neutrons produced in reactors or through spallation reaction were mainly used to study the nuclear reactions, measurement of cross sections and elemental analysis in different materials because of their high neutron flux. Electron accelerator-based neutron sources proving themselves as an attractive alternative to spallation neutron sources because of their compactness, easy handling, adjustable flux, zero radioactive waste, less shielding requirement, etc. Recently low and medium electron accelerators have become very popular to be used for elemental and isotopic identification via neutron resonance spectroscopy [1]. In the current work, the characterization and

optimization of the photo-neutrons produced from the impinging of GeV Class electrons on different metallic targets such as Tungsten (W), Tantalum (Ta) and Lead (Pb) are studied, then compared with that produced from 150 MeV electrons. The angular distribution, mean energy, energy spectrum and nuclear temperature of photo neutrons are evaluated.

### Photo-neutrons production mechanisms

The most common method for producing high gamma fluxes in the Giant Dipole Resonance (GDR) region is the bremsstrahlung process resulting from high energy electrons passing through high Z-materials. This process has a cross

section linear with energy above 20 MeV. The resulting bremsstrahlung spectrum is widely spread in the energy range from zero to the incident energy of electron, and only a small fraction of these photons is "useful" photons, i.e. have energy greater than the binding energy of neutron and lying in the GDR range of  $15 \pm 5$  MeV. Therefore, the overall efficiency of neutron production is much lower than one might expect by having in mind the direct photonuclear process [2]. If the absorbed photon has energy greater than the binding or separation energy of neutron from nucleus, then neutron is emitted. Photonuclear interaction is mainly the result of three specific processes: giant dipole resonance (GDR), quasi-deuteron (QD) production and photo-pion decay. The GDR neutrons are produced by photons at energies ranging from threshold energy to 30 MeV. While at  $50 < E < 140$  MeV, the photoneutron production is due to quasi-deuteron effect (QD). Above 140 MeV, photoneutrons are produced via photo-pion production [3].

#### Monte Carlo MCNP calculations

By using LA150U photonuclear library in Monte Carlo MCNP code, the photonuclear physics has been introduced with photon energies up to 150 MeV [4, 5]. In the current study,  $F_1$  and  $F_5$  tally are used for scoring photo neutrons yield and fluence in different angles.  $10^6$ - $10^7$  histories are run to reduce statistical error less than 5%. Since Monte Carlo MCNP calculations depend sensitively on the simulation geometry, the current simulation results were compared with published data [3, 6] to check the photonuclear physics contained in the code. Figure 1 shows the comparison between the current simulation results and the published data for cylindrical lead target (Pb-207) (thickness 1.68 cm and radius 3 cm), for which the measured data are available.

It is clearly concluded from Fig. (1) that the current simulation results for Lead (pb-207) show a good agreement with the published data.

#### Photo-neutron yield

Photoneutron yield (neutron/s) is calculated for different target thickness and for different electron beam energies by using the following formula [3, 7].

$$\varphi_n = \frac{N_0 \rho t \sigma_t(E)}{M} \varphi_e \quad (1)$$

Here  $M$ ,  $\rho$  and  $t$  are the atomic mass, density and target thickness respectively.  $N_0$  is the Avogadro number,  $\varphi_e$  is the incident electron fluence rate (electron/s),  $\sigma_t(E)$  is the total photonuclear cross-section (the sum of all cross-sections that leads to neutron emission) and  $E$  is the electron incident energy. Figure (2) shows the neutron yield as a function of target thickness for 1 GeV electron beam impinging on Tungsten, Tantalum and Lead targets respectively. Figure (3) shows the neutrons yield produced from 1 GeV and 150 MeV electron energies impinging on Tungsten target.

It is observed from Fig. (2) that as the target thickness increases, the neutron yield increases and saturates beyond the optimized thickness 7.28, 8.5 and 12.35 cm for Tungsten, Tantalum and Lead respectively. Tungsten produces higher photoneutrons yield than Tantalum and Lead [8]. Fig. (3) shows that as the energy of incident electrons increases, the neutrons yield shows a significant increase. The observed increase in neutrons yield may be attributed to the increase of "useful" photons fraction, i.e. photons have energy greater than the binding energy and lying in the GDR or QD ranges [2]. This is, also, due to the increase of electron photon cascaded showers that increase as the electron energy increases. The electron photon cascaded showers can induce photon multiplications in both GDR and QD energy regions. The optimized thickness and the maximum neutrons yield obtained from these targets are listed in Table (1).

Figure (4) shows the forward neutron intensity in comparison with the neutron yield produced from 1 GeV electron energies impinging on Tungsten target. From Fig. (4), it is observed that the majority of neutrons yield is emitted in the outward direction. Also, the neutrons yield emits in forward direction increases as the target thickness increases until certain thickness (60-70 g/cm<sup>2</sup>) then decreases. At certain thickness (60-70 g/cm<sup>2</sup>), almost 23% of the neutron yield is generated in forward direction.

#### Angular distribution of photo-neutrons

Figure (5) shows the angular distribution of neutrons produced from 1 GeV and 150 MeV incident electrons on the optimized thickness of Tungsten target. Figure (6) presents the angular distribution of neutrons produced from 1 GeV incident electrons on different thicknesses of Tungsten

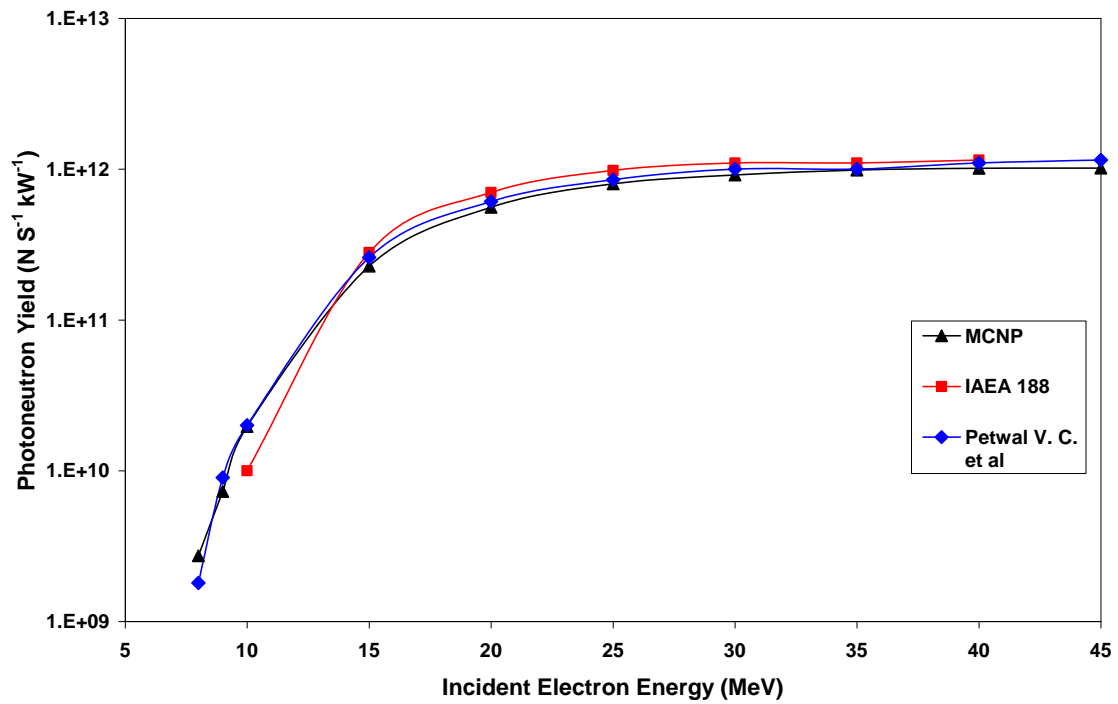


Fig. (1): the photonuclear yield per kW produced from Lead (Pb-207) target (1.68 cm thickness, r=3cm) bombarded to different electron energies

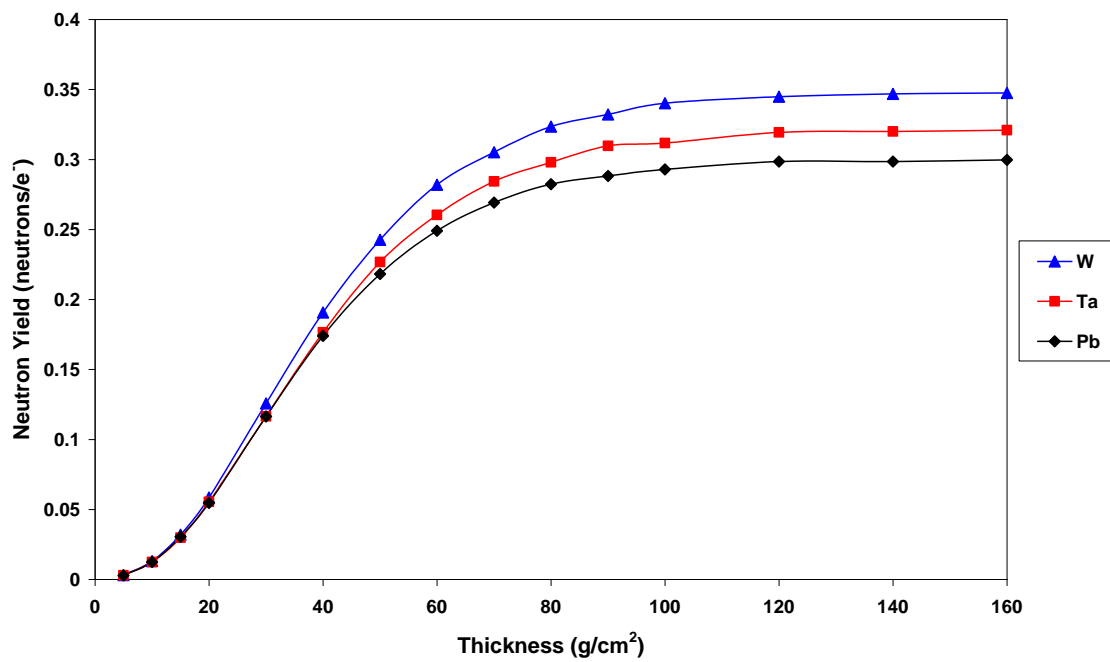


Fig. (2): Neutron yield as function of target thickness for 1 GeV energy electron incident on different targets

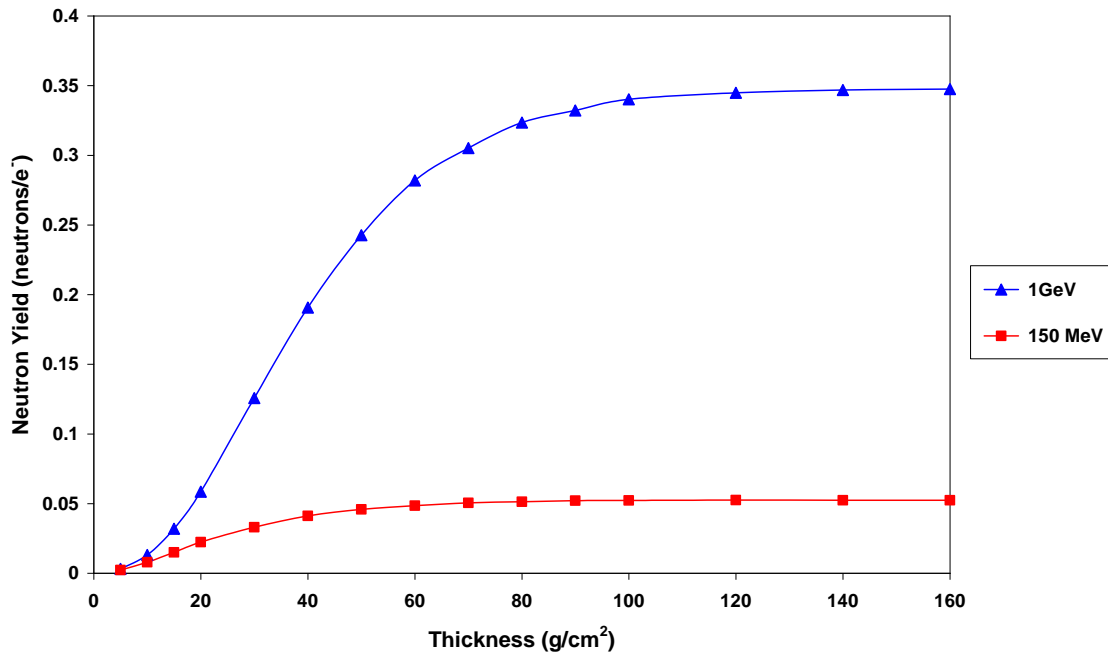


Fig. (3): Neutron yield as function of target thickness for 1 GeV and 150 MeV energy electron incidents on Tungsten targets

Table (1): the maximum neutrons yield at optimize thickness of Tungsten, Tantalum and Lead targets

Target	Electron beam energy	Max. Yield (neutrons/e <sup>-</sup> )	Optimized thickness (g/cm <sup>2</sup> )	Optimized thickness (cm)
Tungsten Z=74, ρ=19.24	1GeV	$3.47 \times 10^{-1}$	140	7.28
	150MeV	$5.23 \times 10^{-2}$	100	5.2
Tantalum Z=73, ρ=16.4	1GeV	$3.2 \times 10^{-1}$	140	8.5
Lead Z=82, ρ=11.34	1GeV	$2.98 \times 10^{-1}$	140	12.35

Figure (5) shows that as the energy of the incident electron decreases, the neutron fluence is almost isotropic [4]. The isotropic nature of neutrons is due to the dominance of GDR neutrons. The neutrons emitted by GDR mechanism are similar to the evaporation neutrons from a compound nucleus [9].

It could be observed from Fig. (6) that for thin targets, the neutrons are produced in an isotropic form. As the target thickness increases

the neutron fluence is assumed to be anisotropic for 1 GeV electrons. The noticed forward-peaked angular distributions may be attributed to the increase of Pre-equilibrium emission of neutrons [4] by increasing the target thickness and due to the anisotropic emission of neutrons from the QD and Photo-Pion decay [9]. Such forward-peaked angular distribution can deliver the highest neutron fluence per cm<sup>2</sup> in forward direction (0 angle).

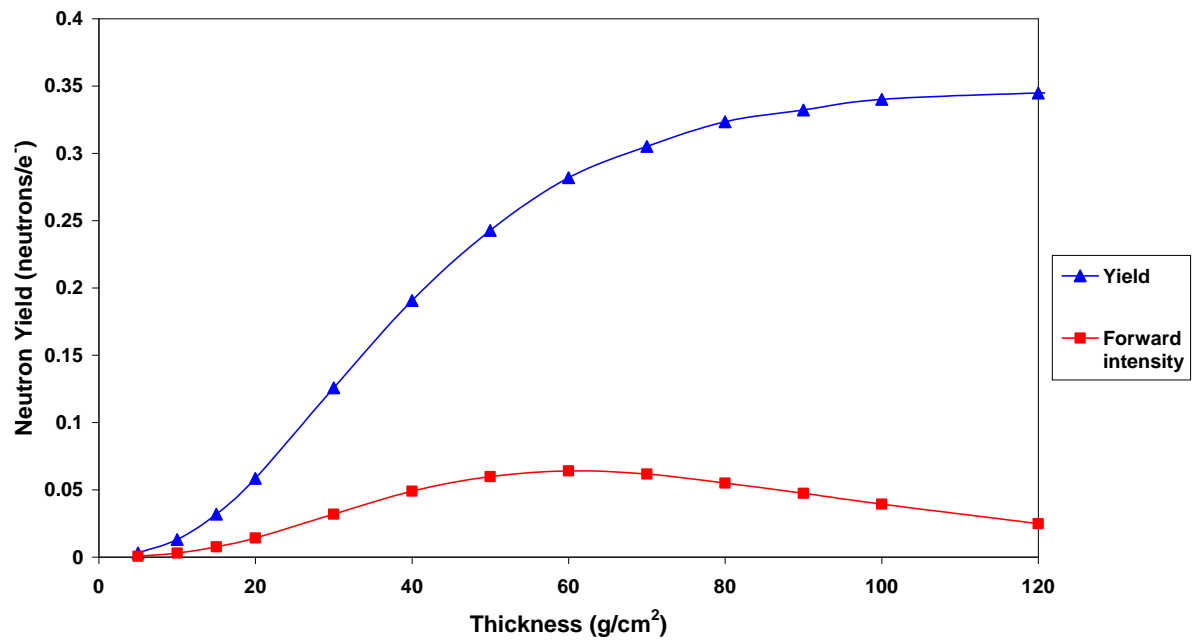


Fig. (4): Neutron yield and forward neutron intensity as function of target thickness for 1 GeV energy electron incidents on Tungsten targets

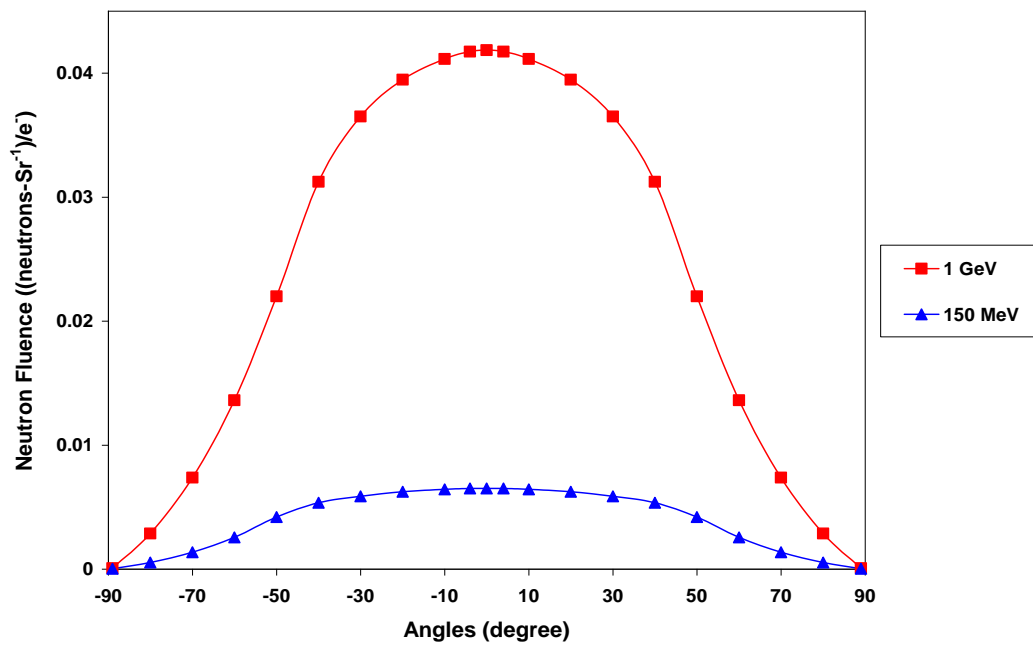


Fig. (5): Angular distribution of neutrons as function of angle for 1 GeV and 150 MeV electron energy incidents on optimized thickness of Tungsten

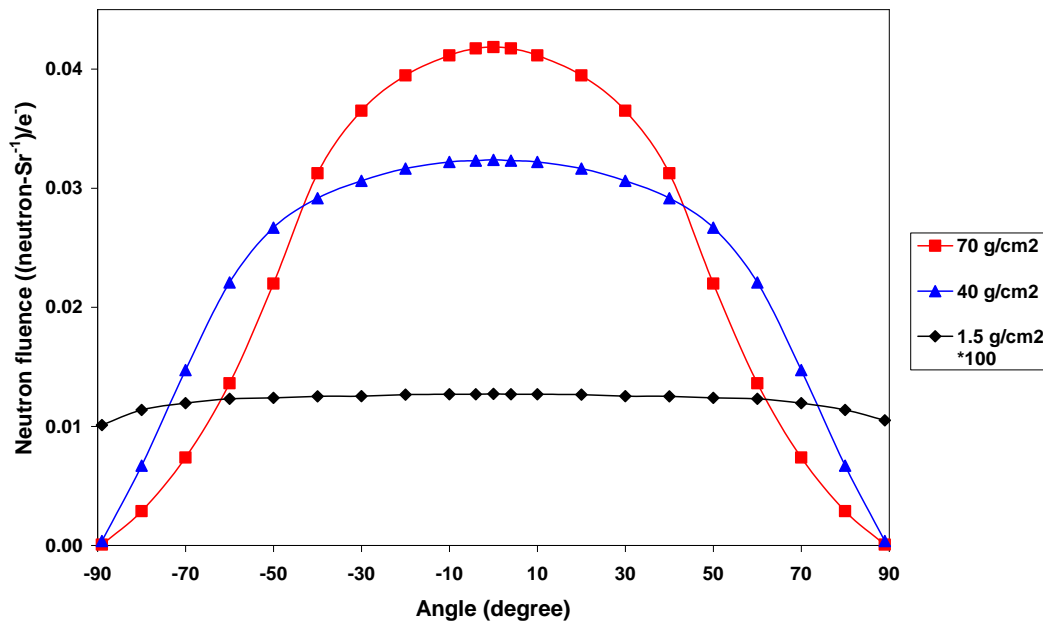


Fig. (6): Angular distribution of neutrons as function of angle for 1 GeV electron energy incidents on different thickness of Tungsten

#### Energy spectrum

Figure (7) shows the energy distribution of neutrons generated from 1 GeV electron beams impinging on Tungsten, Tantalum and Lead targets respectively.

From Fig. (7), the energy spectrum can be well described by a Maxwellian distribution, which is dominated by the low energy neutrons with peak at 0.6, 0.58, 1.2 MeV for Tungsten, Tantalum and Lead targets respectively. The fitted equation of the distribution [3] is:

$$\frac{dN}{dE_n} = k \frac{E_n}{T^2} \exp\left(\frac{-E_n}{T}\right) \quad (2)$$

Here  $T$  is a nuclear temperature (MeV), which is characteristic of a particular target nucleus and represents the most probable energy of the generated neutrons,  $k$  is a normalization factor. From equation fitting the calculated values of the nuclear temperature  $T$  are 0.44, 0.57 and 0.98 MeV for Tungsten, Tantalum and Lead targets respectively [6]. The high nuclear temperature value for lead may be attributed to its high binding or neutron separation energy due to the existence of the magic number (82) in lead nucleus [10].

#### Mean energy of photo-neutrons

The average mean energies of photo-neutrons are 1.64, 1.41 and 2.24 MeV for Tungsten, Tantalum

and lead targets respectively bombarded to 1 GeV electrons and 1.58 MeV for 150 MeV electrons impinging Tungsten. It is observed that Tantalum can produce neutrons with lower mean energy than that for tungsten and lead. The high mean energy of lead may be attributed to the high nuclear temperature ( $T$ ) of lead [10].

#### Conclusion

As a conclusion, the photo-neutron yield increases as the target thickness increases then saturates beyond an optimized thickness of the target. Tungsten produces photo-neutrons more than Tantalum and Lead. Also, the photo-neutron yield shows significant increase as the electron energy increases. At the optimized thickness, the angular distribution of photo-neutrons is found almost isotropic for 150 MeV electrons and anisotropic for 1 GeV electrons. Furthermore, by increasing the electron energy and/or the target thickness, the angular distribution is found to be forward peaked. The energy spectrum of photo-neutrons can be well described by a Maxwellian distribution for both electron energies and the calculated values for nuclear temperature  $T$  are 0.44, 0.57 and 0.98 MeV for Tungsten, Tantalum and Lead targets respectively. Such calculations can help in developing a photo-neutron source-based time of flight facility (TOF) for elemental and isotopic identification via neutron resonance spectroscopy.

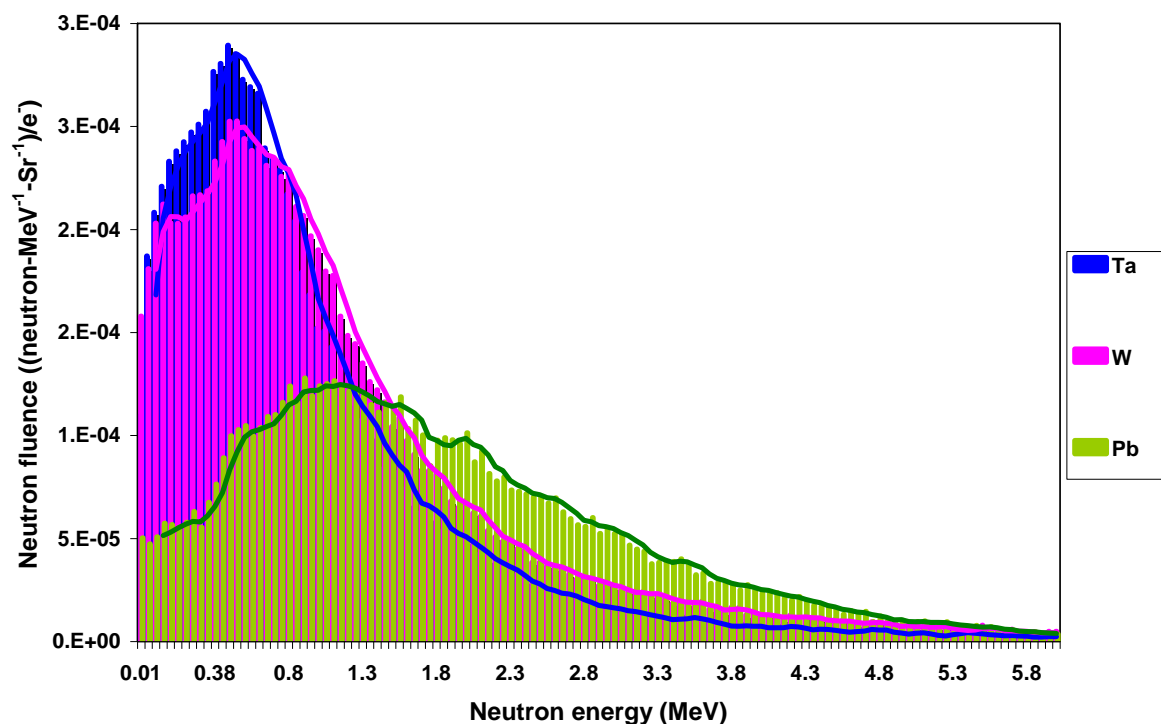


Fig. (7): Energy distribution of neutrons produced from 1 GeV electrons incidents on  $60\text{g/cm}^2$  thickness of different targets

## References

1. Junghans A., (2014): Neutron beams for nuclear data measurements, Neutrons and Nuclei, École Joliot-Curie (EJC), Fréjus, France.
2. Ridikas D., Safa R., Giacri M. L., (2002): Conceptual study of neutron irradiator driven by electron accelerator, 7<sup>th</sup> Information Exchange Meeting on Actinide and Fission Product P&T (NEA/OCDE), Jeju, Korea.
3. Petwal V. C., Senecha V. K., Subbaiah K. V., Soni H. C. and Kotaiah S., (2007): Optimization studies of photo-neutron production in high-Z metallic targets using high energy electron beam for ADS and transmutation, Pramana Journal of Physics, Vol. 68, No. 2, Pp 235-241.
4. X-5 MCNP Team, (2003): A general Monte Carlo N-Particle transport code, version 5, Los Alamos National Laboratory Report, LA-UR-03-1987.
5. Quintieri L., Bedogni R., Buonomo B., Esposito A., De Giorgi M., Mazzitelli G., Valente P. and Gomez-Ros J. M., (2012): Photoneutron source by high energy electrons on high Z target: comparison between Monte Carlo code and experimental data, Transactions of fusion science and technology, Vol. 61, Pp314-421.
6. Swanson W. P., (1979): Radiological safety aspects of the operation of electron linear accelerators, IAEA T R, Technical Report Series No. 188, IAEA.
7. Zolfaghari M. and Sedaghatizadeh M., (2015): Design and Simulation of Photoneutron Source by MCNPX Monte Carlo Code for Boron Neutron Capture Therapy, Iranian Journal of Medical Physics (IJMP), Vol. 12, No. 2, Pp. 129-136.
8. Wasilewski A. and Wronka S., (2006): Monte-Carlo simulations of a neutron source generated with electron linear accelerator, Nukleonika, Vol. 51(3), Pp169-173.
9. Sahani P. K., Haridas G., Sarkar P. K., (2012): simulation of photoneutron spectra due to incident high energy electrons on tungsten target using FLUKA, Indian Journal of Pure & applied physics, Vol. 50, pp. 863-866.
10. Mao X., Kase K. R. and Nelson W. R., (1996): Giant Dipole Resonance neutron yields Produced by electrons as a function of target material and thickness, SLAC-PUB-6628